Separation Science and Technology
Publication details, including instructions for authors and subscription information:
http://www.informaworld.com/smpp/title~content=t713708471

Foam Fractionation Rates

Robert B. Grieves[a]; I. Ugonnaya Ogbu[a]; Dibakar Bhattacharyya[a]; William L. Conger[a]
[a] UNIVERSITY OF KENTUCKY, LEXINGTON, KENTUCKY

To cite this Article Grieves, Robert B. , Ogbu, I. Ugonnaya , Bhattacharyya, Dibakar and Conger, William L.(1970) 'Foam Fractionation Rates', Separation Science and Technology, 5: 5, 583 — 601
To link to this Article: DOI: 10.1080/00372367008055520
URL: http://dx.doi.org/10.1080/00372367008055520

SEPARATION SCIENCE, 5(5), pp. 583–601, October, 1970

Foam Fractionation Rates

ROBERT B. GRIEVES, I. UGONNAYA OGBU,
DIBAKAR BHATTACHARYYA, and WILLIAM L. CONGER
UNIVERSITY OF KENTUCKY
LEXINGTON, KENTUCKY 40506

Summary

An empirical model enables the relation of the batch foam fractionation rate as a power function of the air rate and of the instantaneous residual surfactant concentration, eliminating the bubble size which is difficult to control and to measure. For the cationic surfactant, ethylhexadecyldimethylammonium bromide, the batch foam fractionation rate is directly proportional to the residual surfactant concentration to the first power, except for dilute (<45 mg/liter) solutions, and including suspensions containing colloidal ferric oxide and polynucleated, complexed cyanide. Constants obtained from batch data can be used in the analogue equation for continuous operation to predict accurately the continuous foam fractionation rate, for a single air rate but over a substantial range of feed rates and feed surfactant concentrations. Continuous data from an entirely different column can be fit by a power function equation of the same form, with the power on the effluent or bottoms surfactant concentration again being unity. The accuracy of the predictive equations is in the range 10–18%.

INTRODUCTION

In order to establish the independent variables that influence a foam fractionation process and to determine quantitatively the effect of each independent variable of significance for design purposes, a means of expressing the extent of separation must be adopted. It has been shown in general for foam separations as well as for other partition processes that no single parameter will suffice as the dependent variable to yield the extent of separation. Instead, two parameters must be utilized. One is a *concentration* or *mole fraction* of the

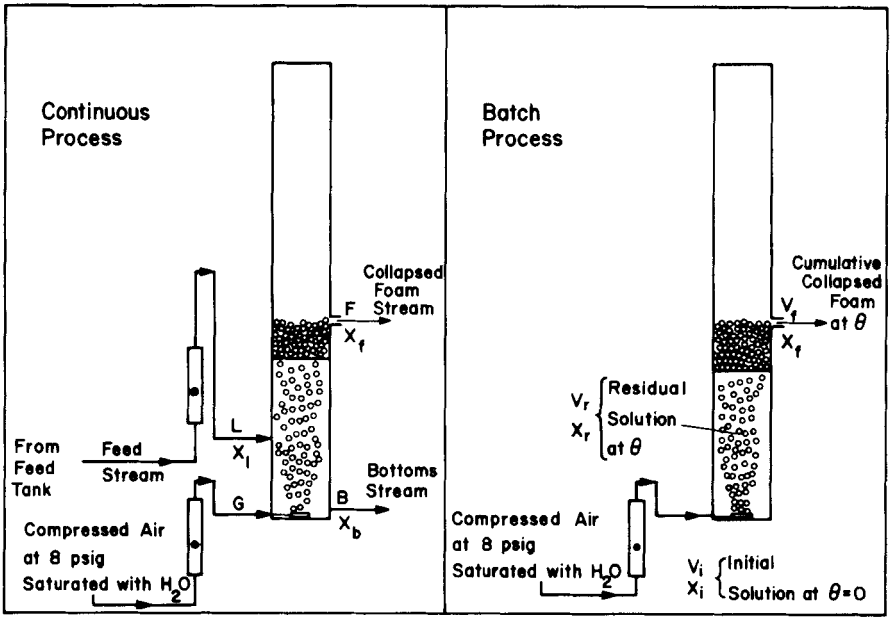

FIG. 1. Schematic diagrams of continuous and batch foam fractionation processes.

component of interest in an effluent stream from the process, and the other is a *quantity* of the component of interest in an effluent stream (*1*). The latter includes the partition of the separating component between the effluent streams together with the relative flow rates (thus including the "inert" or "nonseparating" component) of the effluent streams.

A schematic diagram of a continuous foam fractionation process is shown in Fig. 1a. A surface-active agent, dissolved in the aqueous feed stream, is selectively adsorbed on the surface of gas bubbles that rise through the column, and a foam is formed atop the column of liquid. The foam, in which the surfactant has been concentrated, continuously flows from the fractionation column at a rate F, liter/min, as liquid (collapsed foam), and the bottoms or underflow stream, from which the surfactant has been stripped, flows from the bottom of the column at a flow rate B, liter/min. The following material balances can then be written:

$$L = F + B \tag{1}$$

$$X_l L = X_f F + X_b B \tag{2}$$

in which X_l, X_f, and X_b are the concentrations in mg/liter of surfactant in the appropriate streams. Two of the simplest parameters to indicate the extent of separation are X_b and $X_f F$. The first is to be minimized and the second, the foam fractionation rate, is to be maximized, although it is desirable to achieve the maximization with as low an F and as high an X_f as possible. Of course, other parameters can be used, including reduced concentrations such as X_b/X_l and $(X_l - X_b)/X_l$, and reduced quantities such as $X_f F/X_l L$; or entirely different parameters such as $X_l - X_b$, X_f/X_b, and F/L. A vast array has been presented by the workers in the field of foam separation (*2*).

Batch operation in the laboratory possesses distinct advantages over continuous operation in that small volumes of material can be utilized and experiments can be conducted rapidly, involving time periods of minutes instead of hours for the analogous continuous process. Batch operation is particularly desirable for a feasibility study. A schematic diagram of a batch foam fractionation is shown in Fig. 1b. For the process indicated, the following material balances can be written:

$$V_i = V_f + V_r \tag{3}$$

$$X_i V_i = X_f V_f + X_r V_r \tag{4}$$

It should be noted that there is an inherent disadvantage in that batch operation is nonsteady state, with the liquid level in the column and the foam height, together with the liquid column volume, V_r, and concentration, X_r, changing with time. This could be overcome by recycle of the collapsed foam which would be acceptable for a homogeneous system but unacceptable for a heterogeneous system involving, for example, the microflotation of colloidal particulates. A method of directly relating nonsteady-state batch data toward the design of a continuous flow process would be particularly useful.

The concentration of surfactant in the bottoms stream in a continuous process, X_b, can be determined from the following equation:

$$(X_l - X_b)\frac{L}{G}\frac{D_b}{6000} = \Gamma = -\frac{1}{RT}\frac{d\gamma}{d \ln X_b} \tag{5}$$

in which G is the gas rate, liter/min; D_b is the average bubble diameter, cm; Γ is Gibb's surface excess, mg/cm^2; R is the gas constant,

dyne cm/mg °K; T is the absolute temperature, °K; and γ is the surface tension of the solution of concentration X_b, dyne/cm. Equation (3) can be derived from Gibbs' Equation (*3*) together with Eqs. (1) and (2) (*4–7*). Several assumptions must be made: (a) that the bubbles are spherical; (b) that the liquid column volume (see Fig. 1a) is completely mixed; (c) that the concentration of the liquid draining from the foam is the same as the bulk liquid column concentration, X_b; (d) that dilute solutions are involved; and (e) that a single equilibrium stage separation is achieved, corresponding to equilibrium adsorption in the liquid column plus negligible foam breakage.

The analogous equation for batch operation (see Fig. 1b) can be derived,

$$-\frac{dX_r}{d\theta}\frac{V_i}{G}\frac{D_b}{6000} = \Gamma = -\frac{1}{RT}\frac{d\gamma}{d\ln X_r} \tag{6}$$

V_i, liter, is the initial liquid column volume. The residual liquid column concentration, X_r, mg/liter, can be determined from integration of Eq. (6).

In theory, Γ can be established from surface tension-concentration data for the surfactant solutions and X_b or X_r can thus be calculated from Eqs. (5) or (6) for specified values of the independent variables G, L, X_l, and D_b or G, θ, V_i, X_i, and D_b. However, generally inaccurate results have been obtained (*8*). Instead, Γ can be determined directly in a foam fractionation column, being a function of surfactant and of concentration only. A number of relations between Γ and X_r or X_b have been reported (*2*), generally of the form,

$$\Gamma = a(X_b)^b \tag{7}$$

$$\Gamma = a(X_r)^b \tag{8}$$

For a given surfactant, a and b can vary, depending on the range of X_b. At high values of X_b, $b \to 0$, indicating bubble saturation (*5*). The "constants" a and b are also functions of temperature.

Once Γ is established, the prediction of X_b or X_r should be relatively simple, but this turns out to be not the case: the bubble diameter, D_b, is very difficult to establish experimentally.

(a) D_b varies as the bubbles rise in the column and particularly as the bubbles become part of the foam.

(b) D_b is a function of X_b (or X_r) and of G (*9*).

(c) From commercially-available diffusers, a broad range of bubble

sizes is generally obtained and the range, in turn, may probably change as a function of the period of use.

(d) When utilizing air dissolved in a recycled effluent stream and precipitating the bubbles by depressurizing the stream, the extremely small bubbles (ca. 10 μ) are virtually impossible to measure.

(e) There are numerous experimental hazards in measuring D_b (*10*).

Equations (5) or (6) can be used to predict X_b or X_r, within the limitations indicated. They cannot be used to determine directly the foam fractionation rate, $X_f F$ or $d(X_f V_f)/d\theta$, the other parameter required to determine the extent of separation. An alternate approach is possible, giving reasonably accurate values of the rate of liquid draining from the foam, and thus of F (*2*). But a precise value of D_b is required, together with an experimentally-determined value of the surface viscosity.

The objective of this study is to test an empirical model of a batch foam fractionation process to relate the foam fractionation rate, $d(X_f V_f)/d\theta$, directly to X_r and G, eliminating the need to establish either D_b or the surface viscosity. The relationship which is developed is evaluated over a broad range of surfactant concentrations and of gas rates. The batch relation is then used to predict the foam fractionation rate, $X_f F$, in a continuous process and the predictions are tested experimentally.

EMPIRICAL DEVELOPMENT

In a previous study (*6*), an empirical model has been used to relate X_b to the independent variables, G/L, X_l, and T, for a specified surfactant, column, and gas diffuser. For three surfactants an equation of the form,

$$X_l - X_b = c\left(\frac{G}{L}\right)^d (X_l)^{e/T}(T)^f \tag{9}$$

was derived, and c, d, e, and f were determined. For the batch foam fractionation of surfactants, a simple model has been presented to enable the determination of the qualitative effects of the key independent variables (*11*).

The foam fractionation rate, $X_f F$ or $d(X_f V_f)/d\theta$, consists of two parts: the quantity per unit time of surfactant removed while adsorbed at the gas–liquid interfaces of the bubbles, and the quantity per unit time of surfactant removed in the mechanically entrained liquid car-

ried out of the foam column with the bubbles. The adsorbed surfactant, $X_fF - X_bF$ or $d(X_fV_f - X_rV_f)/d\theta$, can be calculated from Eqs. (1), (2), and (5) or (3), (4), and (6),

$$(X_l - X_b)L = (X_fF - X_bF) = \frac{\Gamma G}{D_b}(6000) \tag{10}$$

$$-\frac{dX_r}{d\theta}V_i = \frac{d(X_fV_f - X_rV_f)}{d\theta} = \frac{\Gamma G}{D_b}(6000) \tag{11}$$

The bubble diameter, at constant gas delivery pressure, should be a function of G and of X_b or X_r. Assuming power functions,

$$D_b = h(G)^j(X_b)^k \tag{12}$$

$$D_b = h(G)^j(X_r)^k \tag{13}$$

with $j > 0$ and $k < 0$ (*9*). From Eqs. (7), (10), and (12) or (8), (11), and (13), and with temperature constant,

$$X_fF - X_bF = 6000ah^{-1}(G)^{1-j}(X_b)^{b-k} \tag{14}$$

$$\frac{d(X_fV_f - X_rV_f)}{d\theta} = 6000ah^{-1}(G)^{1-j}(X_r)^{b-k} \tag{15}$$

The entrained surfactant, X_bF or $d(X_rV_f)/d\theta$, should be a function of X_b or X_r, first because that is the concentration of surfactant in the entrained liquid and second because the viscosity and surface viscosity of the entrained liquid, which affect drainage, are functions of X_b or X_r. The entrained surfactant should also be a function of the superficial velocity of the gas in the column, $G/\Pi r_c^2$, where r_c is the column radius, and of the height, H_f, to which the foam rises above the top of the liquid column before being removed from the foam column. Finally the entrained surfactant should be a function of bubble diameter (*12*) and of temperature. At constant temperature,

$$X_bF = M(X_b)^n(G)(r_c)^{-2}(H_f)^p(D_b)^q \tag{16}$$

$$\frac{d(X_rV_f)}{d\theta} = M(X_r)^n(G)(r_c)^{-2}(H_f)^p(D_b)^q \tag{17}$$

with $n > 0$, $p < 0$, and $q < 0$. For a given foam fractionation column radius at constant foam height and again using Eqs. (12) and (13),

$$X_bF = Mh^q(X_b)^{n+qk}(G)^{1+qj} \tag{18}$$

$$\frac{d(X_rV_f)}{d\theta} = Mh^q(X_r)^{n+qk}(G)^{1+qj} \tag{19}$$

Substituting Eq. (18) into Eq. (14) and Eq. (19) into Eq. (15), the foam fractionation rates are obtained,

$$X_f F = 6000ah^{-1}(G)^{1-j}(X_b)^{b-k} + Mh^q(X_b)^{n+qk}(G)^{1+qj} \quad (20)$$

$$\frac{d(X_f V_f)}{d\theta} = 6000ah^{-1}(G)^{1-j}(X_r)^{b-k} + Mh^q(X_r)^{n+qk}(G)^{1+qj} \quad (21)$$

Because the same two variables appear in both terms on the right-hand sides of Eqs. (20) and (21), it would appear that at least an initial effort should be made to utilize equations simplified by combining the two functions into a single function,

$$X_f F = s(G)^u(X_b)^v \quad (22)$$

$$\frac{d(X_f V_f)}{d\theta} = s(G)^u(X_r)^v \quad (23)$$

thus attempting first to fit $X_f F$ and $d(X_f V_f)/d\theta$ as products of power functions instead of sums of power functions.

EXPERIMENTAL

The batch foam fractionation experiments were carried out at 23°C in a unit schematically diagrammed in Fig. 1b. The Pyrex column was 9.7 cm in diameter and 82 cm in height. Air, saturated with water, was passed through a diffuser of 50 μ porosity at a rate of 78, 115, 168, 195, 264, 340, 440, 660, or 850 ml/min (at 25°C and 1 atm). For each experiment, exactly 2000 ml of surfactant solution, prepared by dissolving ethylhexadecyldimethylammonium bromide (EHDA-Br) in double distilled water (conductivity = 3.9 μmho/cm at 23°C), was placed in the column at $\theta = 0$. EHDA-Br concentrations (X_i) ranged from 12.5 to 280 mg/liter (3.3×10^{-5} to 7.4×10^{-4} M). The pH was maintained at 6.0. The solution was then foam fractionated for a selected time period of 5, 10, 15, 20, 25 or 30 min with foam removed from a foam port located 7.0 cm above the initial liquid column level ($V_i = 2000$ ml). At the termination of each experiment, the residual liquid column volume, V_r, was measured and the concentration of the residual solution, X_r, was determined by a two-phase titration technique using sodium tetraphenylboron as the titrant and bromophenol blue as the indicator (*13*).

The continuous foam fractionation experiments were conducted at 23°C in a unit schematically diagrammed in Fig. 1a. The feed stream containing EHDA-Br (50, 100, or 150 mg/liter) was pumped into a constant head flask and then was metered into the same column as in the batch experiments through a calibrated rotameter at rates of from 0.070 to 0.33 liter/min. The liquid column volume was maintained

at 2000 ml with a foam height of 7.0 cm by means of a liquid-level-controlling tube attached to the column. Steady-state operation was achieved within 1½ to 3 hr, depending on the feed rate. The bottoms stream flow rate, B, and the concentration of surfactant in the bottoms stream, X_b, were then carefully determined. In the continuous experiments, the air rate was maintained at 115 ml/min.

Bubble size was measured in several of the batch experiments by photographing a section of the column directly above the diffuser which contained a wire of known diameter for calibration and then by direct measurement on the enlarged photographic prints.

The photographs were taken with a Nikon camera with a bellow-scope adapter and 35 mm lens. Tri-X film was used at $f/22$ with an electronic flash. From 150 to 250 bubbles were measured on each print and the mean of a normal distribution is reported.

RESULTS AND DISCUSSION

Batch Studies

For each air rate, G, and initial surfactant concentration, X_i, the product of the residual liquid column volume, V_r, and of the residual liquid column concentration, X_r, was plotted vs time and a smooth curve was drawn through the data. The slope of each curve was determined carefully by a graphical technique at every 2.5 min time interval from 0 to 20 min. Longer times were not utilized because the point of no further foam formation was generally reached at 25–30 min. The slopes, $-d(X_rV_r)/d\theta$, were then tabulated vs smoothed values of the residual surfactant concentration, X_r, at identical times. By differentiating Eq. (4) with respect to time,

$$\frac{d(X_fV_f)}{d\theta} = -\frac{d(X_rV_r)}{d\theta} \tag{24}$$

and Eq. (23) can be written as,

$$-\frac{d(X_rV_r)}{d\theta} = s(G)^u(X_r)^v \tag{25}$$

Graphs of the slope, $-d(X_rV_r)/d\theta$, vs X_r at air rates of 264 and 850 ml/min are presented in Fig. 2. Each set of points (a specified symbol) corresponds to a single initial surfactant concentration and foaming times of 0 to 20 min. At the high air rate, a single straight line gives a good fit while at the low air rate, two lines are required.

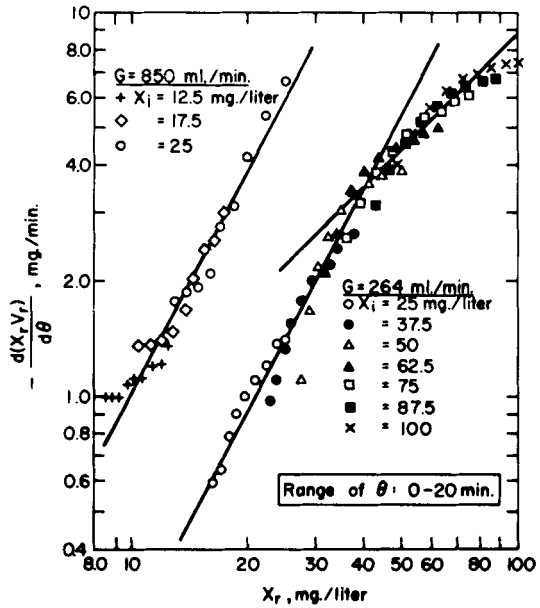

FIG. 2. Batch foam fractionation rates versus residual surfactant concentrations at air rates of 264 and 850 ml/min.

Also, at 264 ml/min each set of points corresponding to an initial surfactant concentration indicates a degree of curvature and a deviation from an equation of the form of Eq. (25). This was produced by the decreasing liquid column volume and increasing foam height at short foaming times, as discussed below. Equation (25) was derived on the basis of constant liquid column volume and foam height.

In order to eliminate this variation, only points with a common liquid column volume of 1900 ml and foam height of 8.2 cm were considered. Thus at each air rate and initial surfactant concentration, the value of $-d(X_rV_r)/d\theta$ and the value of X_r at $V_r = 1900$ ml were determined from the smoothed graphs of the data. This gave a total of 40 points which were then used to determine the constants s, u, and v in Eq. (25). Two equations were necessary to cover the full range of X_r:

10 mg/liter $< X_r <$ 45 mg/liter

$$-\frac{d(X_rV_r)}{d\theta} = 2.90 \times 10^{-6}(G)^{1.17}(X_r)^{2.0} \quad (26)$$

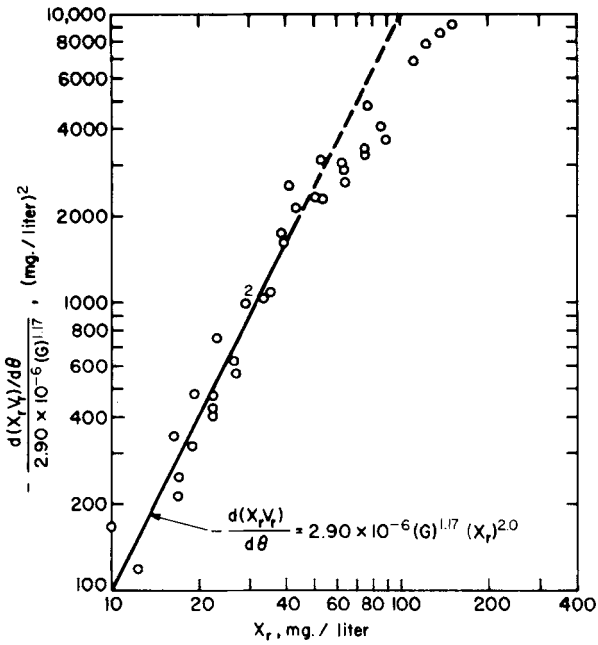

FIG. 3. Test of Eq. (26) for batch foam fractionation at air rates from 115 to 850 ml/min; equation applies to $10 < X_r < 45$. Rates at liquid column volume of 1900 ml.

35 mg/liter $< X_r <$ 300 mg/liter

$$-\frac{d(X_rV_r)}{d\theta} = 1.21 \times 10^{-3}(G)^{0.763}(X_r)^{1.0} \quad (27)$$

The second power on X_r in Eq. (26) and the first power on X_r in Eq. (27) are particularly interesting. An indication of the dependence of the rate on X_r is given in Figs. 3 and 4. The experimentally determined rate divided by $2.90 \times 10^{-6}(G)^{1.17}$ is plotted vs X_r in Fig. 3 with the straight line of slope = 2.0 giving values predicted by Eq. (26). The experimentally determined rate divided by $1.21 \times 10^{-3}(G)^{0.763}$ is plotted vs X_r in Fig. 4, with the straight line of slope = 1.0 giving values predicted by Eq. (27). It is clear that little variation in the slopes from values of 1.0 and 2.0 could be permitted. It is also clear that a definite transition occurs for 35 mg/liter $< X_r <$ 45 mg/liter and that a single equation could not cover the full range of X_r. It is most likely that the transition was produced by a change in the value

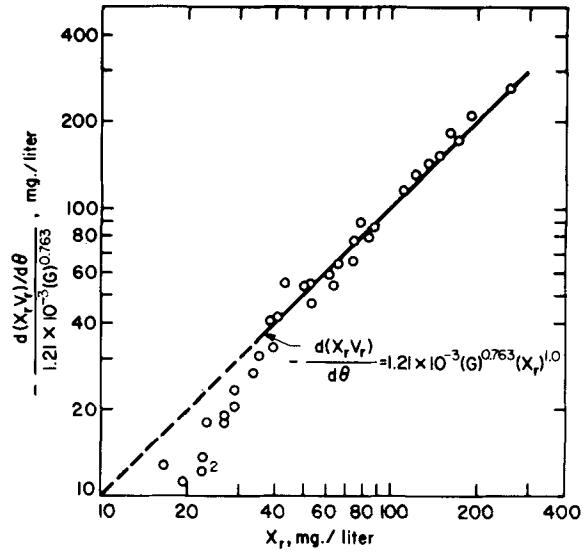

FIG. 4. Test of Eq. (27) for batch foam fractionation at air rates from 78 to 850 ml/min. Equation applies to $35 < X_r < 300$. Rates at liquid column volume of 1900 ml.

of b in Eq. (8) or by a change in k in Eq. (13). Other than in this transition region, there is a remarkable constancy in the power on X_r.

For 21 data points in the range 10 mg/liter $< X_r <$ 45 mg/liter, the average per cent deviation of values of $-d(X_rV_r)/d\theta$ calculated with Eq. (26) from experimental values is 19.1%. Average per cent deviation is defined as

$$\sum_{\text{no. of points}} \frac{|\text{experimental-calculated}|}{\text{experimental}} \times 100/\text{no. of points}$$

For 23 data points in the range 35 mg/liter $< X_r <$ 300 mg/liter, the average per cent deviation of values of $-d(X_rV_r)/d\theta$ calculated with Eq. (27) from experimental values is 7.3%.

As noted above, Figs. 3 and 4 and Eqs. (26) and (27) apply to a constant liquid column volume of 1900 ml and foam height of 8.2 cm. Variation in liquid column height and foam height produced virtually no variation in the powers u and v in Eq. (25) but did produce changes in s. In general, s increased as the liquid column volume decreased from 2000 to 1900 ml (and as the foam height in-

creased from 7.0 to 8.2 cm) and then any further increase was slight, with s remaining essentially constant. This can be observed from the data shown in Fig. 2 at $G = 264$ ml/min. This initial decrease was probably produced by start-up effects: as the liquid column volume began to drop from 2000 ml at $\theta = 0$ for each experiment, anomalous behavior would be expected as the foam began to rise and to wet the glass column and until the foam began to leave at the foam removal port. Once the foam was flowing steadily the anomaly disappeared. The values of $-d(X_rV_r)/d\theta$ at $\theta = 0$ were obtained by careful data extrapolation, but the extrapolation would not eliminate the anomaly. From the data in Fig. 2 at $G = 850$ ml/min; the variation in s with liquid column height and foam height was eliminated at the higher air rates (this also held at $G = 660$ and 440 ml/min and almost at 340 ml/min) due to the more rapid rise of the foam to the removal port. An additional series of experiments with $V_i = 3450$ ml, instead of 2000 ml, and with the initial foam height at 7.0 cm, showed that the height of the liquid column did not have a significant effect on the foam fractionation behavior, and Eqs. (26) and (27) remained applicable for $V_r = 3350$ ml (analogous to 1900 ml and 8.2 cm foam height above). This provided validation for the control of the process by adsorption and the achievement of equilibrium.

Bubble size measurements were made at 2.5 min intervals from 2.5 to 20 min for three series of experiments, at $G = 264$ ml/min and $X_i = 50$ mg/liter; at $G = 264$ ml/min and $X_i = 100$ mg/liter; and at $G = 440$ ml/min and $X_i = 40$ mg/liter. The purpose was principally to report the magnitude and range of bubble sizes encountered in the experimental phase of the work. The average of the mean bubble sizes for each series, together with the average of the standard deviations, is given in Table 1. As would be expected, bubble size decreased as G was decreased and as X_i was increased. Of course, during each series of experiments, D_b increased with time as X_r decreased. Referring to Eq. (13), the power k could be determined for each series with G held constant and is presented in Table 1. In all three cases the power

TABLE 1

	$G = 264$, $X_i = 50$	$G = 264$, $X_i = 100$	$G = 440$, $X_i = 40$
Average of mean D_b, μ	360	260	430
Average of standard deviation, μ	110	100	120
Value of k in Eq. (13)	−0.6	−0.9	−0.4

relation indicated by Eq. (13) was quite valid. In comparing the first and third series, k does not appear to be entirely independent of G. Further bubble size measurements might have been made at different values of G and X_i and correlated by Eq. (13). However, the purpose of the development of Eqs. (22) and (23) was to eliminate D_b from consideration, because it is not effectively at the control of the design engineer. In addition, the bubble sizes that were established were at a fixed, single position in the column and did not necessarily represent the true, available interfacial area. For each measurement, a broad range of bubble sizes was found.

Previous studies have been made of the foam separation of negatively charged colloidal ferric oxide (*14*) and of cyanide complexed by ferrous iron, polynucleated $[FeFe(CN)_6]^{2-}$ (*15*), both utilizing EHDA-Br and batch experiments. Fundamental attention was paid to the foam separation rates of the particulates of interest, although measurements were also made of surfactant concentrations. The rates of foam separation of EHDA-Br for these studies are given in Figs. 5 and 6, which are analogous to Fig. 2 for the foam fractionation of pure EHDA-Br. For each study, the air rate was held constant, but

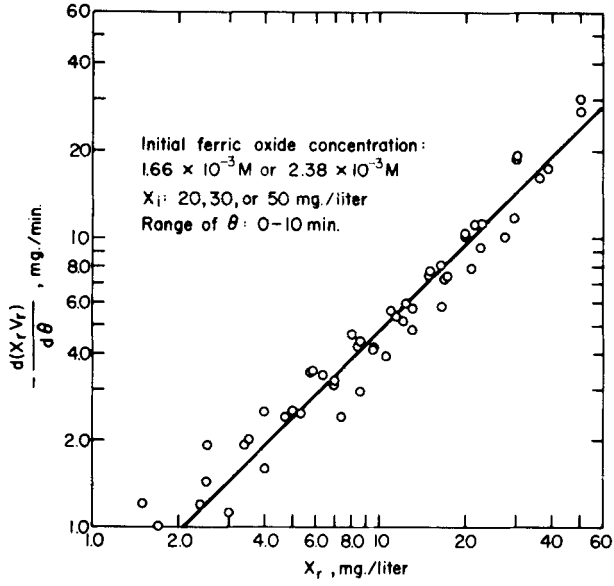

FIG. 5. Batch foam fractionation rates vs residual surfactant concentrations at gas rate of 1300 ml/min in presence of negatively-charged colloidal ferric oxide at pH 10.8.

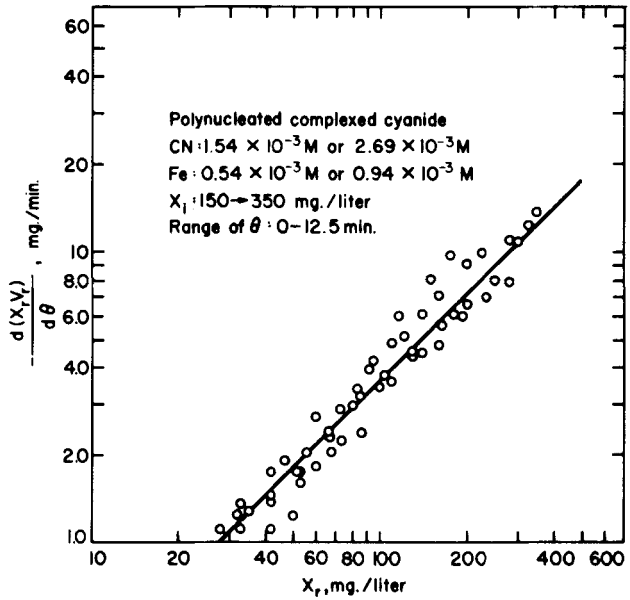

FIG. 6. Batch foam fractionation rates vs residual surfactant concentrations at gas rate of 1440 ml/min in presence of polynucleated complexed cyanide at pH 7.0.

the initial surfactant concentration was varied. In both cases, except at very low values of X_r at close to foam cease, a line of unity slope gives a good fit. This yields a value of unity for v in Eq. (25). In comparing the data of Figs. 2, 4, and 5, it should be stressed that entirely different mechanisms of surfactant foam separation were operative. With the ferric oxide, part of the EHDA-Br was removed adsorbed on the particulate surfaces in nonstoichiometric quantities, while with the complexed cyanide, part of the EHDA-Br was removed stoichiometrically associated with the polynucleated complex ions.

Continuous Studies

To test the applicability of the numerical values of the constants in Eq. (23) to the continuous analogue, Eq. (22), for predicting the continuous foam fractionation rate, $X_f F$, a series of continuous experiments was carried out in the same column as that in which the batch studies were made. A single air rate of 115 ml/min was employed, but the feed surfactant concentration, feed rate, and height of liquid column (at

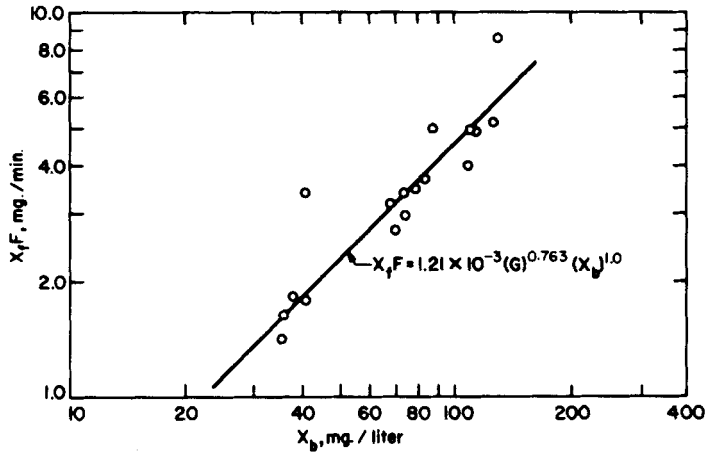

FIG. 7. Continuous foam fractionation rates vs bottoms surfactant concentrations at air rate of 115 ml/min, with predicted line from continuous analogue of Eq. (27).

constant foam height) were varied. Results are presented in Fig. 7 with X_fF related to X_b. The line is established from Eq. (27), with X_b in the appropriate range. An adequate job of predicting the continuous results is done by the continuous analogue of Eq. (27).

The average per cent deviation of values calculated with Eq. (27) from experimental values was 11.9% for the 17 points. A value of unity for the power v is clearly validated. The liquid column height was also varied in the continuous experiments, at constant air rate, feed surfactant concentration, and foam height. There was no detectable change in the separation, either in X_b or in X_fF. This again indicated that adsorption of the surfactant at the bubble interfaces was the controlling process and that an equilibrium separation was achieved. It should be stressed again that in comparing the batch and continuous results, the same foam fractionation column, diffuser, etc. were employed.

Extensive continuous foam fractionation data have been gathered in previous studies (*16*) in order to determine the effects of the independent variables on X_b and F. The data never have been used to test an equation of the form of Eq. (22). Accordingly, 19 data points for EHDA-Br with the ranges of the independent variables given below, were used to establish Eq. (28):

Foam height = 74 cm
Liquid column height = 102 cm
X_l = 100, 200, 400 mg/liter
L = 0.025, 0.050, 0.10 liter/min
G = 600, 1030, 1600, 2090 ml/min

$$X_f F = 5.50 \times 10^{-5}(G)^{1.02}(X_b)^{1.0} \tag{28}$$

Results are presented in Fig. 8, with the experimental values of $X_f F$ divided by $5.50 \times 10^{-5}(G)^{1.02}$ plotted vs X_b, and the straight line of slope = 1.0 giving values predicted by Eq. (28). The first power on X_b is validated. The average per cent deviation from experimental values of values of $X_f F$ calculated with Eq. (28) is 18.4% for 19 points. The wide discrepancy in the values of s and v, comparing Eqs. (28) and (27), was obviously produced by the contrasting air diffusers, columns, and foam heights employed in the two sets of experiments.

Equation (28) could be used together with the equation,

$$X_b = X_l - 0.0419(X_l)^{0.78}\left(\frac{G}{L}\right)^{0.37} \tag{29}$$

which had been developed previously (*6*) to eliminate X_b and relate $X_f F$ to the independent variables G, X_l, and L.

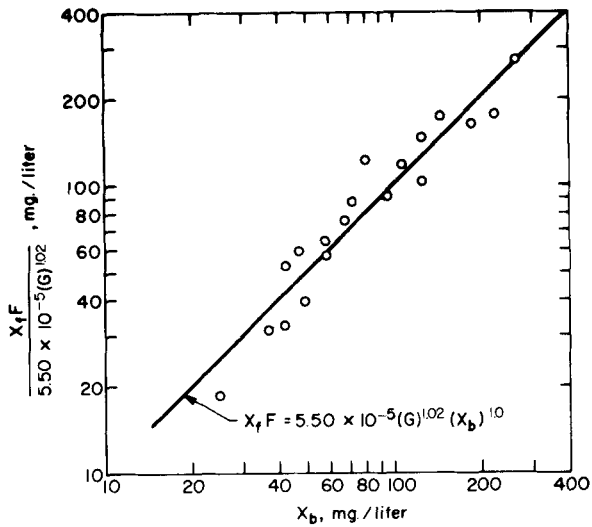

FIG. 8. Test of $(X_b)^{1.0}$ in Eq. (28) for continuous foam fractionation at air rates from 600 to 2090 ml/min.

CONCLUSIONS

An empirical model has been developed, relating the foam fractionation rate in a batch process to the air rate and instantaneous residual surfactant concentration,

$$-\frac{d(X_r V_r)}{d\theta} = s(G)^u(X_r)^v$$

eliminating the bubble size, which is an important variable but difficult to determine and to control. A series of batch experiments yielded values of v of 2.0 for low values of X_r (<45 mg/liter) and of 1.0 for high values of X_r (>35 mg/liter). The transition may have been produced by variation in the equilibrium adsorption relation and/or by variation in the relation between bubble size and X_r, changing the interfacial area and/or the foam drainage. A limited number of bubble size measurements was made. The transition also produced a change in the dependence of $-d(X_r V_r)/d\theta$ upon G. Data from other batch studies with the same surfactant, but involving the foam separation of colloidal ferric oxide and polynucleated complexed cyanide, could be fit by the same relation, both with a value of v of 1.0. The expected accuracy of the batch equations was about 10–15%.

The foam fractionation rate for continuous experiments, conducted in the same column at a single air rate but at variable feed concentration, feed rate, and liquid column height, could be accurately predicted from the equation,

$$X_f F = s(G)^u(X_b)^v$$

with s, u, and v *established entirely from batch data.* The accuracy was about 12%. Extensive, continuous foam fractionation data, with the same surfactant but an entirely different column and range of air rates, could be fit accurately by an equation of the same form, with $v = 1.0$ and $u = 1.02$. The accuracy of the equation was about 18%.

The empirical model has been validated and has enabled the prediction of continuous foam fractionation rates from batch rate data for a single stage separation. Further experimental validation of batch predictions of continuous results should be made over a broader range of air rates and for several surfactants.

Nomenclature

B flow rate of bottoms or effluent stream from continuous process, liter/min

D_b	bubble diameter, μ or cm
F	flow rate of foam stream (collapsed, as liquid) from continuous process, liter/min
G	air or gas rate, ml/min [except for Eqs. (5) and (6) liter/min]
H_f	height of foam above top of liquid column, cm
L	flow rate of feed stream to continuous process, liter/min
R	gas constant, dyne cm/mg °K
r_c	radius of foam fractionation column, cm
T	temperature, °K
V_f	volume of foam (collapsed, as liquid) accumulated in θ min from batch process, liter
V_i	initial volume of liquid for each batch experiment, liter
V_r	volume of residual liquid in liquid column after θ min in batch process, liter
X_b	surfactant concentration in bottoms or effluent stream from continuous process, mg/liter
X_f	surfactant concentration in foam stream from continuous process or in accumulated foam from batch process, mg/liter
X_l	surfactant concentration in feed stream to continuous process, mg/liter
X_r	surfactant concentration in residual liquid column volume from batch process, mg/liter
$a, b, c, d, e, f, h, j, k, m, n, p, q, s, u, v$	coefficients or powers
γ	surface tension, dyne/cm
Γ	Gibbs' surface excess, mg/cm^2
θ	batch foam fractionation time, min

REFERENCES

1. P. R. Rony, *Separ. Sci.*, **3**, 239 (1968).
2. R. Lemlich, *Ind. Eng. Chem.*, **60**(10), 16 (1968).
3. J. W. Gibbs, *Collected Works*, Longmans Green, New York, 1928.
4. D. L. Banfield, I. H. Newson, and P. J. Alder, *Amer. Inst. Chem. Eng.—Inst. Chem. Eng.* (London) *Symp. Series*, **1**, 3 (1965).
5. I. H. Newson, *J. Appl. Chem.* (London), **16**, 43 (1966).
6. R. B. Grieves and D. Bhattacharyya, *J. Water Poll. Control Fed.*, **37**, 980 (1965).

7. R. K. Wood and T. Tran, *Can. J. Chem. Eng.*, **44,** 322 (1966).
8. D. L. Banfield, M. P. Simpson, I. H. Newson, and P. J. Alder, *Surface Excess in Solutions of Surface-Active Agents: I. A Comparison of Static and Dynamic Results,* AERE-R 5124, Atomic Energy Research Establishment. Harwell, Berk, England, 1966.
9. V. Kevorkian, *Foam Separation,* Ph.D. thesis, Columbia University, New York, 1958.
10. B. L. Karger and D. G. DeVivo, *Separ. Sci.*, **3,** 393 (1968).
11. R. B. Grieves, *Brit. Chem. Eng.*, **13,** 77 (1968).
12. P. F. Wace, P. J. Alder, and D. L. Banfield, *Chem. Eng. Progr. Symp. Series #91,* **65,** 19 (1969).
13. J. T. Cross, *Analyst,* **90,** 315 (1965).
14. R. B. Grieves and D. Bhattacharyya, *J. Appl. Chem.* (London), **18,** 149 (1968).
15. R. B. Grieves and D. Bhattacharyya, *J. Appl. Chem.* (London), **19,** 115 (1969).
16. R. B. Grieves and R. K. Wood, *Amer. Inst. Chem. Eng. J.*, **10,** 456 (1964).

Received by editor March 9, 1970